ACS APPLIED MATERIALS & INTERFACES

Research Article

www.acsami.org

Fluorescent Ensemble Based on Bispyrene Fluorophore and Surfactant Assemblies: Sensing and Discriminating Proteins in Aqueous Solution

Junmei Fan, Liping Ding,* Yu Bo, and Yu Fang

Key Laboratory of Applied Surface and Colloid Chemistry of Ministry of Education, School of Chemistry and Chemical Engineering, Shaanxi Normal University, Xi'an 710062, P. R. China

Supporting Information

ABSTRACT: A particular bispyrene fluorophore (**1**) with two pyrene moieties covalently linked via a hydrophilic spacer was synthesized. Fluorescence measurements reveal that the fluorescence emission of **1** could be well modulated by a cationic surfactant, dodecyltrimethylammonium bromide (DTAB). Protein sensing studies illustrate that the selected ensemble based on **1**/DTAB assemblies exhibits ratiometric responses to nonmetalloproteins and turn-off responses to metalloproteins, which can be used to differentiate the two types of proteins. Moreover, negatively charged nonmetalloproteins can be discriminated from the positively charged ones according to the difference in ratiometric responses. Fluorescence sensing studies with control bispyrenes indicate that the polarity of the spacer connecting two pyrene moieties plays an important role in locating bispyrene fluorophore in DTAB assemblies, which further influences its sensing behaviors to noncovalent interacting proteins. This study sheds light on the influence of the probe structure on the sensing performance of a fluorescent ensemble based on probe and surfactant assemblies.

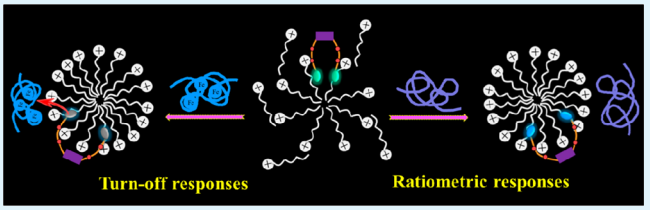

KEYWORDS: *supramolecular assemblies, DTAB, fluorescent sensor, nonmetalloprotein, metalloprotein*

1. INTRODUCTION

Surfactants, block copolymers, and amphiphilic dendrimers usually self-assemble into dynamic, heterogeneous, nanoscale supramolecular assemblies such as micelles, liposomes, and vesicles in aqueous solutions.[1,2] The hydrophobic microdomains formed by hydrocarbon tails can noncovalently encapsulate guest fluorophores and enhance their solubility,[3] fluorescence stability,[4] and quantum yield[5] in aqueous solution. Moreover, surfactant assemblies can tune the photophysical properties[6] and fluorescence emission behaviors of the encapsulated fluorescent probe,[7−9] which can be used to sense external stimuli such as the pH and chemicals that induce changes of surfactant assemblies.[10] Therefore, supramolecular assemblies encapsulating fluorophores have been widely used to develop fluorescent sensors because this method reduces their dependence on molecular design and synthesis and enables aqueous detection. A great number of fluorescent ensembles based on fluorophores/surfactant assemblies have been developed as sensors for detecting various analytes, such as metal ions,[11−15] anions,[3,16,17] amino acids,[8,18,19] and explosives.[20−22]

Detection of proteins is of great significance because proteins are involved in the diagnosis of various affiliated diseases including Alzheimer's, Huntington's, Parkinson's, and prion diseases.[23−25] Surfactant assemblies encapsulating fluorophores provide a more simple and convenient way to develop label-free fluorescent sensors to proteins because these ensemble sensors are based on the noncovalent interaction between proteins and surfactant assemblies. Thayumanavan and co-workers have endeavored to use this strategy to develop fluorescent sensors or arrays for proteins, where they reported using micellar assemblies based on amphiphilic polymers,[26] polyelectrolyte and surfactant mixtures,[27,28] and amphiphilic dendrimers[29] to encapsulate small fluorophores. In these reports, fluorescence quenching signals were observed because the encapsulated fluorescent guests were released into aqueous solution because of the disassembly of the supramolecular assemblies induced by protein binding. Ji et al. used a similar strategy to realize turn-off detection of heparin-binding proteins such as protamine and Tat peptide, where they used micellar assemblies based on cationic surfactant and bioactive polyanion heparin to encapsulate pyrene.[30] Binding with protamine or Tat peptide leads to the disassembly of micelles and then the release of pyrene into aqueous solution with decreased fluorescence intensity. Although these supramolecular ensembles have shown interesting sensing behaviors to proteins, the developed fluorescent ensembles for proteins are still limited and new ensembles and novel strategies are highly demanded.

More recently, we introduced a new simple and cost-effective approach to develop fluorescent aqueous sensors for proteins,

Received: July 21, 2015
Accepted: September 28, 2015
Published: September 28, 2015

DOI: 10.1021/acsami.5b06604
ACS Appl. Mater. Interfaces 2015, 7, 22487−22496

where the sensing platform was built using only commercially available surfactant rather than mixtures of surfactant with polyelectrolytes/dendrimers or bioactive polyanions to encapsulate small fluorophores.[31] Moreover, this strategy provides a novel sensing mechanism, where the fluorophore probes the aggregation changes of surfactant assemblies upon protein binding. The developed ensemble based on a cholesterol-modified pyrene-based fluorophore and dodecyltrimethylammonium bromide (DTAB) assemblies shows selective ratiometric responses to pepsin and O-egg over a series of tested proteins.

In the present work, we intend to develop novel fluorescent ensembles based on new small fluorophores and surfactant assemblies for sensing proteins and to evaluate the influence of the fluorophore structure on the interaction with surfactant assemblies and thereafter on the sensing performance of the obtained ensemble. Therefore, a particular neutral bispyrene-based fluorophore (**1**; Scheme 1) was designed and synthesized

Scheme 1. Synthesis Route of the Bispyrene Fluorophore 1

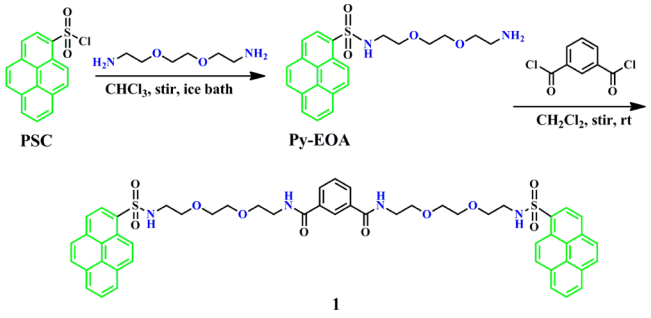

to be used as the probe, where the two pyrene moieties are connected to the benzene ring via a hydrophilic oligo(oxyethylene) spacer. The ensemble based on the **1**/DTAB assembly exhibits ratiometric responses to the noncovalently bound nonmetalloproteins and turn-off responses to metalloproteins. This label-free supramolecular fluorescent sensor can discriminate metalloproteins from nonmetalloproteins and differentiate negatively charged nonmetalloproteins and positively charged ones. Examination of the fluorescent ensembles based on four control bispyrene compounds reveals that the structure of the probe plays an important role in the sensing performance of supramolecular ensembles.

2. EXPERIMENTAL SECTION

Reagents and Instruments. Pyrene (Alfa, 98%) was used after recrystallization by ethanol. Isophthaloyl dichloride (J&K, 98%) and 1,8-diaminooctane (J&K, 98%) were used as supplied. 2,2-(Ethylenedioxy)bis(ethylamine) (EOA; 98%), dodecyltrimethylammonium bromide (DTAB; ≥98%), and all proteins including pepsin (PS; from porcine gastric mucosa, lyophilized powder, P7012), bovine serum albumin (BSA; lyophilized powder, A1933), ovalbumin (O-egg; from chicken egg white, lyophilized powder, A5503), *β*-lactoglobulin (BLG; from bovine milk, lyophilized powder, L3908), trypsin (TPS; from bovine pancreas, lyophilized powder, T1426), lysozyme (LYZ; from chicken egg, lyophilized powder, L6876), cytochrome *c* (Cyt C; from bovine heart, lyophilized powder, C2037), and ferritin (Ferr; from equine spleen, type I, saline solution, F4503) were purchased from Sigma-Aldrich Co. and used as received. 2X *N*-(2-hydroxyethyl)-piperazine-*N*-ethanesulfonic acid (HEPES) buffer solution (42 mM, pH 7.4) was purchased from Beijing Solarbio Science & Technology Co., Ltd., and used as diluted to a constant concentration (10 mM, pH 7.4). The stock solutions of various proteins were prepared separately in 10 mM HEPES buffer (pH 7.4) and stored at 0−4 °C. Analytically pure trichloromethane was dried with anhydrous $CaCl_2$ overnight before use. Dichloromethane and trimethylamine were distilled before reaction. All aqueous solutions were prepared from Milli-Q water (18.2 MΩ cm at 25 °C), and all other reagents were analytically pure.

The melting point was measured on a X5 microscopic melting point meter (Beijing Tech Instrument). The ^1H and ^{13}C NMR spectra of the synthesized chemicals were obtained on a Bruker Avance 400 MHz NMR spectrometer. The high-resolution mass spectrometry (MS) spectra were acquired in electrospray ionization (ESI) positive mode using a Bruker Maxis UHR-TOF mass spectrometer. The Fourier transform infrared (FTIR) spectra were measured on a FTIR spectrometer (Vertex 70v, Bruker, Germany). Steady-state fluorescence measurements were conducted on a single-photon-counting fluorescence spectrometer (FS5, Edinburgh Instruments, UK) with xenon light (150 W) as the excitation source, and the excitation and emission slit widths were set at 2 and 1.5 nm, respectively. All samples were excited at 350 nm. Time-resolved fluorescence measurements were conducted on the time-correlated single-photon-counting fluorescence spectrometer (FLS920, Edinburgh Instruments, UK). All of the solutions were excited by a laser (343.4 nm), and the emission wavelength was fixed at 500 nm. The particle size distribution and scattering intensity (count rate) were measured on a Malvern Zetasizer Nano-ZS90.

Synthesis of the Bispyrene Fluorophore 1. The synthesis route of the target bispyrene fluorophore **1** is depicted in Scheme 1. The starting material, pyrenesulfonyl chloride, was synthesized by adopting a literature method.[32] The synthesis of Py-EOA was described in detail in our previously reported work.[33] The synthesis and purification of

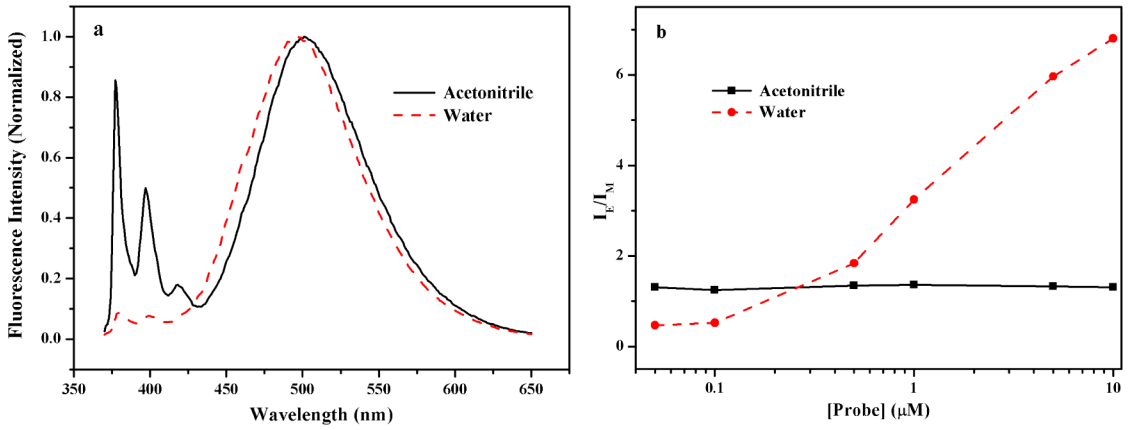

Figure 1. (a) Fluorescence emission spectra of **1** (1.0 μM) in acetonitrile and water (λ_{ex} = 350 nm). (b) Fluorescence intensity ratio of excimer to monomer (I_E/I_M) of **1** in acetonitrile and water as a function of the probe concentration varying from 0.05 to 10 μM.

DOI: 10.1021/acsami.5b06604
ACS Appl. Mater. Interfaces 2015, 7, 22487−22496

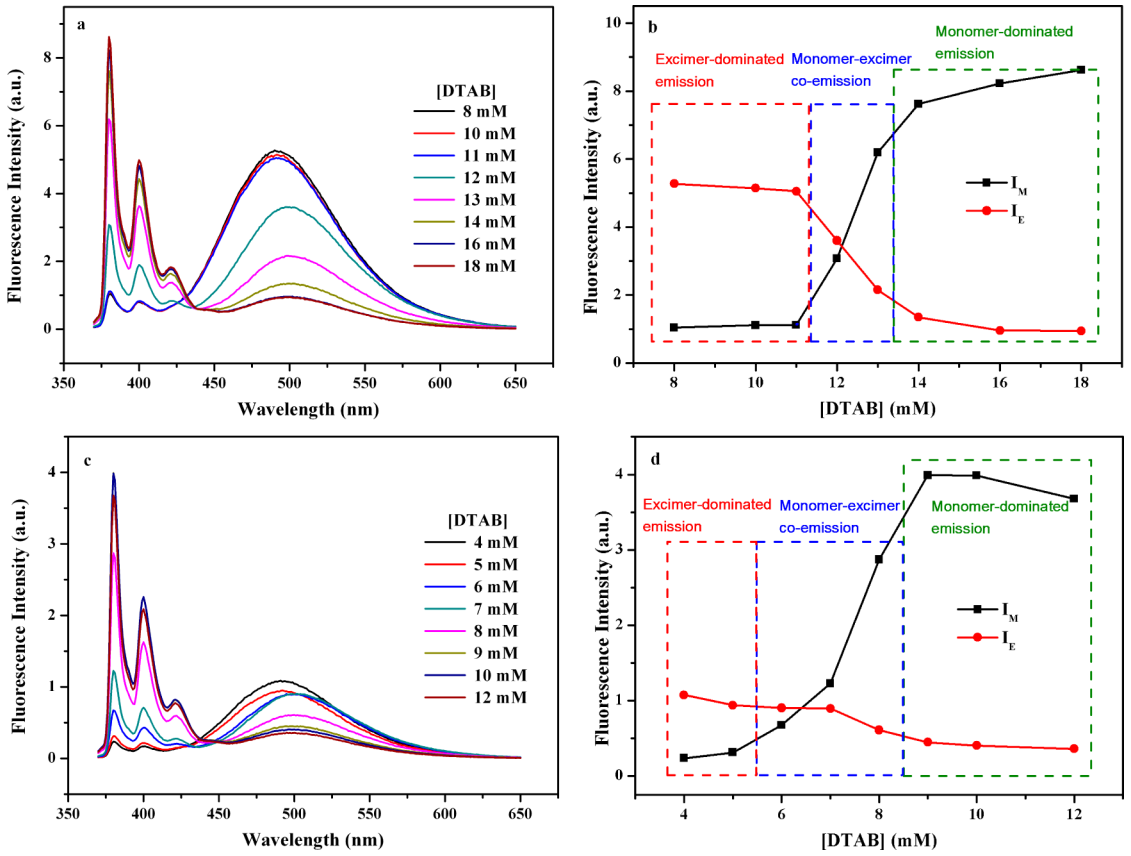

Figure 2. (a) Fluorescence emission spectra of **1** (1.0 μM) in a series of different concentrated DTAB solutions in water. (b) Fluorescence intensities of monomer at 381 nm and excimer at 500 nm of **1** (1.0 μM) as a function of the DTAB concentration in water. (c) Fluorescence emission spectra of **1** (1.0 μM) in different concentrated DTAB buffer solutions (10 mM HEPES, pH 7.4). (d) Fluorescence intensity of monomer at 381 nm and excimer at 500 nm of **1** (1.0 μM) as a function of the DTAB concentration in HEPES buffer solution (10 mM, pH 7.4).

the target bispyrene-based fluorophore, **1**, is as follows: A solution of isophthaloyl dichloride (0.122 g, 0.6 mmol, 1 equiv) in CH_2Cl_2 (20 mL) was added dropwise to a solution of Py-EOA (0.504 g, 1.2 mmol, 2 equiv) and triethylamine (184 μL, 1.32 mmol, 2.2 equiv) in 50 mL of CH_2Cl_2 at 0 °C under argon, after which the reaction system was stirred at room temperature for 48 h. Then the mixture was washed with brine until the pH of the aqueous layer was neutral. The organic layer was dried over anhydrous Na_2SO_4 and purified by column chromatography (CH_2Cl_2:CH_3OH = 10:1, v/v). The final product, **1**, was obtained as a pale-yellow foamy solid (0.5142 g, 89.7%). Mp: 86.6−87.1 °C. ^{1}H NMR (400 MHz, $CDCl_3$, ppm): δ 8.95 (d, J = 9.4 Hz, 1H), 8.66 (d, J = 8.2 Hz, 1H), 8.31−8.00 (m, 7H), 7.90 (dd, J = 7.8 and 1.6 Hz, 1H), 7.28 (t, J = 5.9 Hz, 1H), 7.23 (s, 1H), 6.36 (s, 1H), 3.65−3.49 (m, 4H), 3.38 (dd, J = 11.5 and 5.6 Hz, 6H), 3.13 (d, J = 4.6 Hz, 2H). ^{13}C NMR (101 MHz, $CDCl_3$, ppm): δ 166.79, 134.67, 134.26, 131.33, 130.75, 130.39, 130.10, 129.96, 129.89, 128.74, 127.95, 127.04, 126.90, 126.82, 126.76, 125.13, 125.03, 123.79, 123.78, 123.15, 70.16, 70.05, 69.78, 69.22, 42.94, 39.91. IR (KBr plates, cm^{-1}): 3300 (−NH−), 2923 (−CH_2−), 3048 (Ar−H), 1700 (C═O), 1590 (Ar C═C), 1145 (O═S═O), 1098 (C−O−C). HS-MS (ESI; [M + Na]$^+$). Calcd for $C_{52}H_{50}N_4O_{10}S_2$: 977.2861. Found: 977.2865.

3. RESULTS AND DISCUSSION

Fluorescence Emission of Bispyrene 1 in Neat Solvents. The steady-state emission spectra of **1** (1.0 μM) were examined in good (acetonitrile) and poor (water) solvents. As shown in Figure 1a, the fluorophore exhibits strong excimer emission centering at about 500 nm in both solvents but shows considerably different monomer emissions. In acetonitrile, the structured monomer emission is comparative to the excimer emission; however, in water, the monomer emission is extremely smaller than the excimer emission. The studies of the concentration effect of the probe reveal that the ratio of excimer-to-monomer emission is independent of the concentration of the probe in acetonitrile but highly concentration-dependent in water (Figures 1b and S1 in the Supporting Information), indicating the formation of an intramolecular excimer in the good solvent and an intermolecular excimer in the poor solvent.[34] Such results suggest that the fluorophore can be well dissolved in the good solvent but aggressively aggregate in the poor solvent.

DTAB Concentration Effect on the Fluorescence Emission of Bispyrene 1. The modulation effect of DTAB aggregates on the fluorescence emission of **1** was evaluated in both nonbuffered and buffered aqueous solutions. Similar results were found in both media, where the concentration of DTAB has a remarkable effect on the profile of the emission spectra of the probe (Figure 2a,c). For both cases, the conformation of the probe went through three stages, as depicted by the comparison of monomer and excimer emission intensities with increasing DTAB concentration. As illustrated in Figure 2b,d, first, in lowly concentrated DTAB solutions, the probe emits excimer-dominated emission, with the excimer intensity being much larger than that of monomer emission, which suggests that the bispyrene molecules aggregate tightly just like in the poor solvent, second, with increasing DTAB concentration, the probe exhibits monomer−excimer coemission because the intensity of excimer decreases remarkably with

DOI: 10.1021/acsami.5b06604
ACS Appl. Mater. Interfaces 2015, 7, 22487−22496

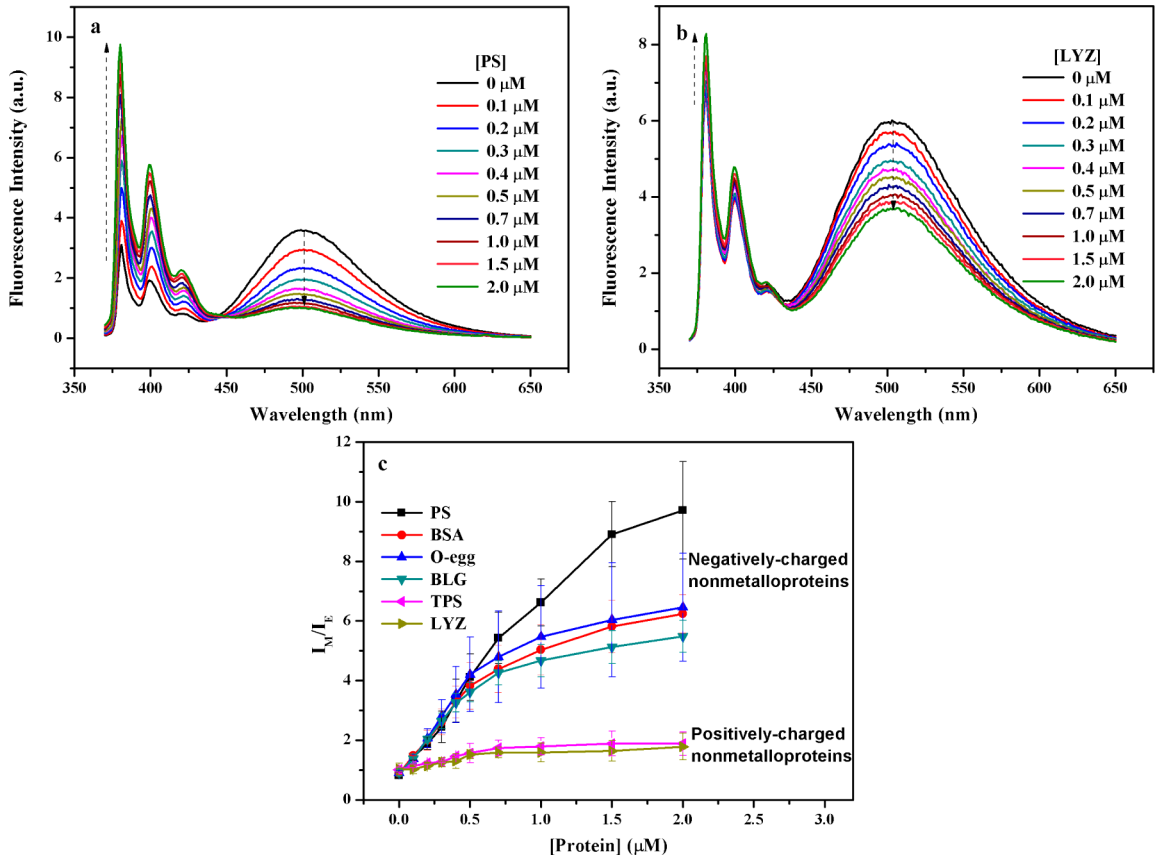

Figure 3. Fluorescence emission spectra of **1**/DTAB (1.0 μM/6 mM) in HEPES buffer solution (10 mM, pH 7.4) upon the addition of (a) PS and (b) LYZ. (c) The ratio of monomer-to-excimer intensity (I_M/I_E) of the ensemble of **1**/DTAB (1.0 μM/6 mM) as a function of the protein concentration. Each value is an average of three parallel measurements.

concomitant enhancement of the monomer intensity, suggesting that fluorophore aggregates can be disrupted by the gradually formed surfactant assemblies, and third, in highly concentrated DTAB solutions, the probe emits nearly total monomer emission, with the monomer emission being conversely and remarkably larger than the excimer emission, indicating that the two pyrene moieties are separated from each other.

The big difference between in nonbuffered and buffered solutions is that the turning point for the three stages occurs at different DTAB concentrations. This could be due to the different aggregating behaviors of DTAB molecules in the two solutions because HEPES buffer introduces more complex ingredients (cf. Figure S2 in the Supporting Information). One thing to be noted is that the turning point for the probe changing from monomer−excimer coemission to monomer-dominated emission in a nonbuffered aqueous solution is at a concentration of 14 mM DTAB, which is the critical micellar concentration of DTAB in neat water. These results suggest that DTAB micelles benefit the stretching of two pyrene moieties of the probe and lead to monomer emission. In the case of buffered solutions, the critical point of changing from excimer-dominated emission to excimer−monomer coemission is observed at a concentration of 6 mM DTAB. Further increasing DTAB concentration will lead to total monomer emission, which occurs at 9 mM DTAB. As we learned from our previous studies, the protein binding may facilitate further aggregation of DTAB assemblies and induce the probe to go through changes from one emission state to another,[31] which is dependent on the adopted DTAB concentration. Therefore, 6 mM DTAB was selected to incorporate the present probe to construct a fluorescent ensemble for sensing proteins because the probe exhibits monomer−excimer coemission in this DTAB solution, which may easily change forward to monomer-dominated emission or backward to excimer-dominated emission.

Sensing Behaviors of 1/DTAB Assemblies for Nonmetalloproteins in HEPES Solution. The ensemble based on **1**/DTAB assemblies shows greatly enhanced fluorescence stability in aqueous solution than the probe itself (Figure S3 in the Supporting Information), indicating its possible application in aqueous detection. We first measured the sensing behaviors of **1**/DTAB assemblies to six nonmetalloproteins, including PS (p*I* 1.0), BSA (p*I* 4.7), O-egg (p*I* 4.7), BLG (p*I* 5.1−5.3), TPS (p*I* 10.5), and LYZ (p*I* 11.0). These nonmetalloproteins can be divided into two types: one is negatively charged proteins, with p*I* being below physiological pH, and the other is positively charged proteins, with p*I* being above 7.4. Interestingly, the fluorescence responses to these two types of proteins are quite different, although ratiometric responses were observed for both cases. For negatively charged proteins including PS, BSA, O-egg, and BLG, the ratiometric response is presented as a remarkably enhanced monomer emission accompanied by a significantly decreased excimer emission with increasing protein concentration (Figures 3a and S4a−c in the Supporting Information). The emission state of the probe changes from monomer−excimer coemission to monomer-dominated emission with an isoemissive point at 445 nm, suggesting

DOI: 10.1021/acsami.5b06604
ACS Appl. Mater. Interfaces 2015, 7, 22487−22496

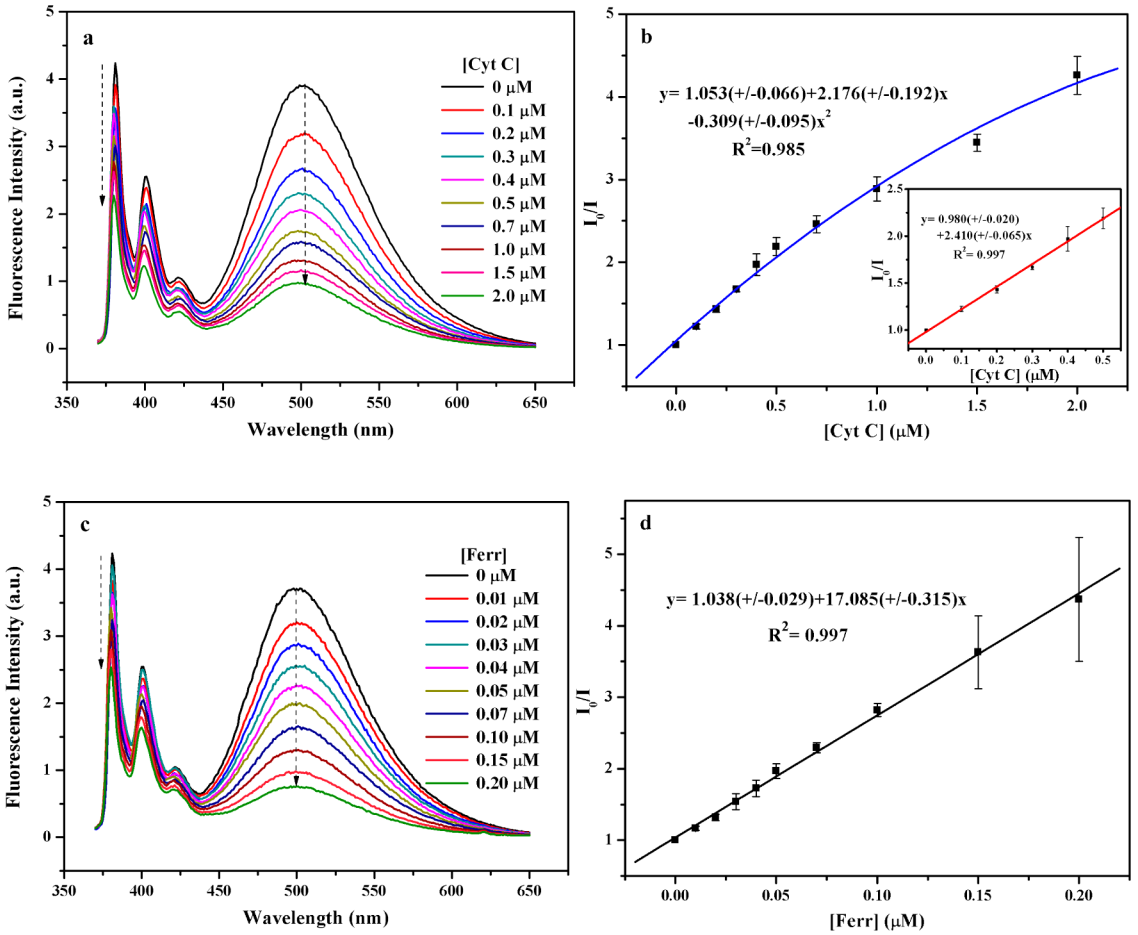

Figure 4. (a) Fluorescence emission spectra of **1**/DTAB (1.0 μM/6 mM) in HEPES buffer solution (10 mM, pH 7.4) upon the addition of Cyt C. (b) Fluorescence quenching plot (I_0/I) of **1**/DTAB over the concentration of Cyt C (inset: linear relationship between I_0/I and the Cyt C concentration below 0.5 μM). (c) Fluorescence emission spectra of **1**/DTAB (1.0 μM/6 mM) in HEPES buffer solution (10 mM, pH 7.4) upon the addition of Ferr. (d) Fluorescence quenching plot (I_0/I) of **1**/DTAB over the concentration of Ferr. The error bars stand for the standard deviation of three measurements.

transformation between two molecular conformations. For positively charged proteins like LYZ and TPS, the ratiometric response is presented with much smaller extent of monomer enhancement and excimer reduction with increasing protein concentration, where the emission state of the probe stays at excimer−monomer coemission (Figures 3b and S4d in the Supporting Information).

As illustrated in Figure 3c, the sensor system exhibits a remarkable increase of the fluorescence intensity ratio of monomer to excimer, I_M/I_E, to the four tested negatively charged nonmetalloproteins over a concentration ranging from 0 to 2.0 μM, while it shows a slight enhancement of I_M/I_E to the two measured positively charged nonmetalloproteins over the same concentration range. The I_M/I_E values are closely related to the p*I* values of proteins that increase in the order of PS (1.0), BSA (4.7), O-egg (4.7), BLG (5.1−5.3), TPS (10.5), and LYZ (11.0). The lower the p*I* values are, the more negative charges the protein bears, the bigger the I_M/I_E values appear upon the addition of the protein, especially when the protein concentration is above 0.5 μM. Such results indicate that the electrostatic interaction between proteins and DTAB assemblies plays an important role in the process of sensing nonmetalloproteins.

Sensing Behaviors of 1/DTAB Assemblies for Metalloproteins in HEPES Solution. We then measured the sensing behaviors of **1**/DTAB assemblies to metalloproteins including Cyt C (p*I* 10.7) and Ferr (p*I* 4.5). Both of these two metalloproteins have metal cofactors that could accept energy or charge from the excited state of the fluorophores.[26,35] In this regard, it is easy to understand the turn-off response observed for these two metalloproteins. As seen in Figure 4a,c, the fluorescence emission of the supramolecular ensemble decreases continuously upon titration of Cyt C and Ferr. As displayed in Figure 4b,d, the plots of I_0/I are linear over the low concentration range of proteins and the concentration-dependent quenching behaviors follow the Stern−Volmer equation (1):

$$I_0/I = 1 + K_{sv}[Q] \quad (1)$$

where I_0 and I are the excimer intensity of the **1**/DTAB ensemble at 500 nm in the absence and presence of different concentrations of quencher, i.e., metalloproteins. K_{sv} denotes the Stern−Volmer constant and can be extracted from the plots of I_0/I versus [Q]. For Cyt C, a linear plot emerges at low concentrations ranging from 0 to 0.5 μM (inset of Figure 4b), and the K_{SV} value is calculated as 2.41 ($\pm$0.07) × 10^6 M^{-1}. We have also measured the K_{SV} value at low concentrations of Ferr. As shown in the inset of Figure 4d, the superlarge K_{SV} value, 1.71 ($\pm$0.32) × 10^7 M^{-1}, represents higher sensitivity to Ferr than to Cyt C.

DOI: 10.1021/acsami.5b06604
ACS Appl. Mater. Interfaces 2015, 7, 22487−22496

Pattern Recognition of Different Types of Proteins by 1/DTAB Assemblies. The versatile fluorescence responses of the present supramolecular ensemble toward differently charged nonmetalloproteins and metalloproteins may enable it to provide recognition patterns for different types of proteins. Therefore, the logarithm data of fluorescence variation (I/I_0) for both monomer and excimer emissions were collected for different proteins. For enhanced fluorescence, a positive signal provided as $\log(I/I_0)$ is larger than 0; on the contrary, for quenched fluorescence, a negative signal obtained as $\log(I/I_0)$ is smaller than 0. Figure 5 illustrates the response patterns of the

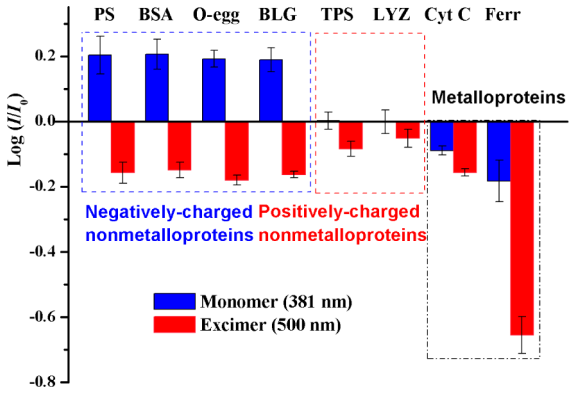

Figure 5. Recognition patterns for proteins (0.2 μM) by collecting fluorescence variation of monomer and excimer emissions. Each value is an average of three parallel measurements.

fluorescent ensemble to the three types of proteins (0.2 μM). Differential responses for different proteins reveal analyte-specific patterns. For nonmetalloproteins, there are both fluorescence enhancement and quenching. The values of $|\log(I/I_0)|$ of both monomer and excimer for negatively charged nonmetalloproyeins are much larger than those for positively charged nonmetalloproteins, which is the key that can distinguish between these two types of proteins. For metalloproteins, the turn-off response mode with both negative signals can discriminate them from nonmetalloproteins. Thus, the present fluorescent ensemble provides a simple way of discriminating nonmetalloproteins and metalloproteins by presenting different response modes. This is advantageous compared to the reported supramolecular ensemble based on a polymer−surfactant complex that can discriminate metallo- and nonmetalloproteins only at the nanomolar level by presenting different extents of fluorescence quenching but cannot differentiate them at a micromolar concentration because they produce similar quenching responses because of the disassembly of the polymer−surfactant complex.[28] The fluorescence responses to some metal ions were also measured to check the possible influences from metal ions. As shown in Figure S5 in the Supporting Information, the sensor ensemble displays very small fluorescence quenching responses to a series of metal ions including Fe^{3+}, Cu^{2+}, Co^{2+}, Zn^{2+}, Ni^{2+}, Ca^{2+}, Mg^{2+}, Cd^{2+}, Pb^{2+}, and Ba^{2+} even at a concentration 10 times that of proteins. Moreover, the previously observed multiple responses to these metal ions by bispyrene fluorophores in SDS assemblies are not found here (Figure S6 in the Supporting Information).[36] Therefore, the cationic surfactant ensemble can function as responsive sensors to proteins without interference from metal ions.

Sensing Mechanism of a Fluorescent Ensemble to Metalloproteins. The observed quenching responses to metalloproteins could be mainly due to the energy/electron transfer from the surfactant-assembly-encapsulated fluorescent probe to metalloproteins because this phenomenon has been extensively reported for sensing metalloproteins.[37−40] The possibility of fluorescence quenching induced by the disassembly of the surfactant assembly is ruled out by dynamic light scattering (DLS) measurements, where the size of the supramolecular ensemble is retained or increased upon the addition of metalloproteins (Figure S7 in the Supporting Information). Time-resolved fluorescence decays were also measured to explore the quenching mechanism. As illustrated in Figure S8 in the Supporting Information and Figure 6, the decay curves barely change and the lifetime ratio, τ_0/τ, nearly equals 1 upon an increase in the concentration of both metalloproteins, where τ_0 and τ represent the lifetime of the sensor system in the absence and presence of metalloproteins, respectively. Such results suggest that the quenching by these two metalloproteins is static in nature, indicating the binding of metalloproteins with the sensor system.[41] The higher quenching efficiency of Ferr than that of Cyt C could be due to the larger binding interaction of Ferr with DTAB assemblies because Ferr (p*I* 4.5) carries negative charges at neutral pH. The larger increase of the ensemble size by Ferr than by Cyt C

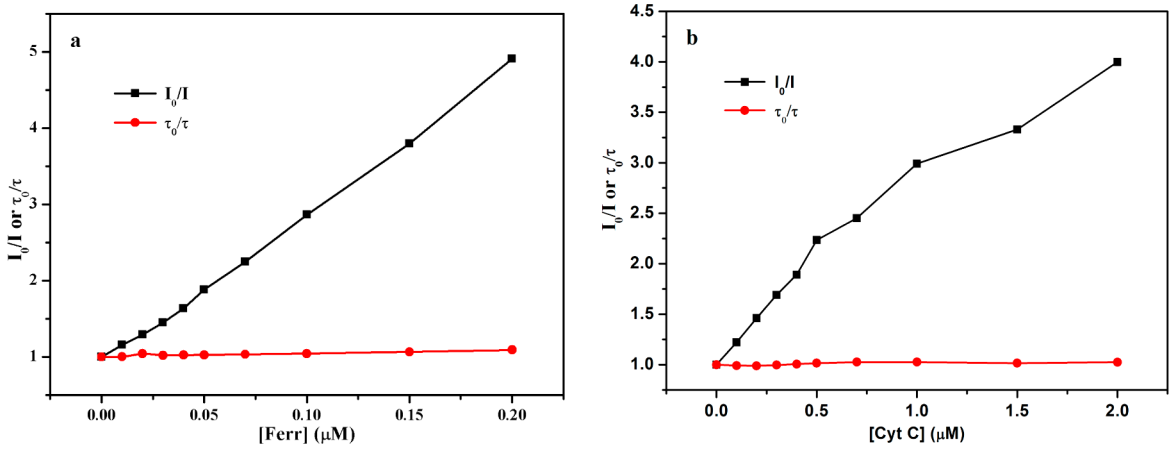

Figure 6. Quenching plots of the fluorescence intensity ratio (I_0/I) and the fluorescence lifetime ratio (τ_0/τ) of **1**/DTAB (1.0 μM/6 mM) to the concentration of Ferr (a) and Cyt C (b).

DOI: 10.1021/acsami.5b06604
ACS Appl. Mater. Interfaces 2015, 7, 22487−22496

proves this assumption (inset of Figure S7 in the Supporting Information).

Sensing Mechanism of a Fluorescent Ensemble to Nonmetalloproteins. The observed ratiometric responses to nonmetalloproteins could be due to the protein-binding-induced aggregation changes of DTAB assemblies as observed in our previous study,[31] which, in turn, affect the molecular conformation of the bispyrene probes in the surfactant assemblies. Therefore, we measured the DLS and Tyndall effects to estimate the size variation of the ensemble aggregate in the presence of various proteins. As illustrated in Figure 7,

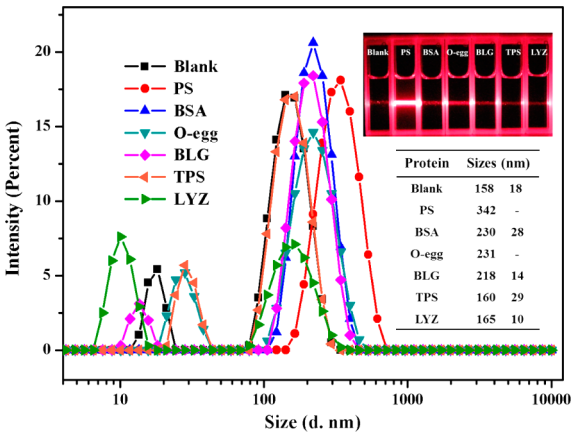

Figure 7. Size distribution of **1**/DTAB (1.0 μM/6 mM) before and after the addition of various proteins (0.5 μM). Inset: photographs of the Tyndall effect of **1**/DTAB upon the addition of various proteins (0.5 μM).

the main size of the sensor aggregate prior to the addition of proteins is ca. 158 nm, accompanied with smaller size aggregates (ca. 18 nm). Upon the addition of 0.5 μM nonmetalloproteins including PS, BSA, O-egg, BLG, TPS, and LYZ, the size of the sensor ensemble changes to 342, 230, 231, 218, 160, and 165 nm, respectively. Clearly, the lower the p*I* value of the protein is, the higher is the increase of the aggregate size that is observed. Similarly, a more apparent Tyndall effect was witnessed for the addition of proteins with low p*I* values such as PS, BSA, and O-egg (inset of Figure 7). This could be understood because the lower p*I* value endows the protein with more negative charges at neutral pH and a resulting stronger electrostatic interaction with DTAB assemblies.[42] The trend in the increase of the assembly size is in accordance with the extent of ratiometric responses induced by these nonmetalloproteins, verifying that the aggregation changes of the sensor assembly are accountable for the ratiometric responses. The earlier studies of the DTAB concentration effect on the fluorescence emission of the probe reveal that the changes of the DTAB assemblies from premicelle to micelle facilitate the fluorescence emission varying from monomer−excimer coemission to monomer-dominated emission (cf. Figure 2a,c). Therefore, it is more likely that the addition of nonmetalloproteins changes the sensor platform from a loosely aggregated assemble to a micelle-like one.

Molecular Structure Effect of Bispyrenes on the Sensing Performance of Fluorescent Ensembles to Proteins. It is worth noting that the currently observed quenching responses to metalloproteins and ratiometric responses to other nonmetalloproteins such as BSA and BLG were not observed in our previous sensor system based on monopyrene fluorophore/DTAB assemblies, which exhibit only ratiometric responses to PS and O-egg.[31] The multiple sensing behaviors of the present supramolecular ensemble could be due to the use of bispyrene fluorophores and the different locations of the probe in DTAB assemblies. The effective quenching of the present ensemble by metalloproteins suggests that the location of probe **1** in DTAB assemblies is accessible to the added proteins, which is more likely at the interface between the surfactant assembly and aqueous solution. This is possible because a polar spacer is used to connect the two pyrene moieties.

To evaluate the role of spacer polarity between the two pyrene moieties in the sensing process, we particularly synthesized a control bispyrene fluorophore, **2**, with the same length but a hydrophobic spacer (Scheme S1 in the Supporting Information). We first measured the DTAB concentration effect on its fluorescence emission in HEPES buffer solution. It displays similar fluorescence variation from excimer-dominated emission to monomer−excimer coemission and then to monomer-dominated emission with increasing DTAB concentration (Figure S9 in the Supporting Information). The difference is that the DTAB concentration for **2** to emit monomer−excimer coemission is at 7 mM rather than at 6 mM for **1**. Then, we examined the protein sensing behaviors of two ensembles based on **2**/ DTAB assemblies: one is with 6 mM DTAB like the sensor system based on **1**, and the other is with 7 mM DTAB, exhibiting monomer−excimer coemission similar to that of **1** with 6 mM DTAB. Interestingly, both control ensembles exhibit quite different sensing behaviors compared to **1**/DTAB, where the ratiometric responses to non-metalloproteins and turn-off responses to metalloproteins are much smaller (Figures S10 and S11 in the Supporting Information). These results indicate that the hydrophilic structure between the two pyrene moieties in **1** indeed plays an important role in the multiple sensing behaviors of detecting proteins.

To deeply understand the effect of the spacer polarity on the sensing performances, we further examined fluorescent ensembles based on three more control bispyrene compounds with different spacer lengths: two with hydrophilic spacers also containing oxyethylene units (**1A** and **1B**) and one with a hydrophobic spacer containing only methylene units (**2A**). The structures of **1A**, **1B**, and **2A** are shown in Scheme S2 in the Supporting Information, and the synthesis of these molecules was reported in our previous work.[36] Interestingly, both **1A** and **1B** are found to start to emit monomer−excimer coemission in 6 mM DTAB as probe **1** does, whereas **2A** is found to display such an emission in 7 mM DTAB, as probe **2** does (Figure S12 in the Supporting Information). Then, the sensing behaviors of the five fluorescent ensembles that all exhibit monomer−excimer coemission were measured and compared. The results are shown in Figure S13 in the Supporting Information. It can be seen that either for the ratiometric responses to non-metalloproteins (Figure S13a,b in the Supporting Information) or for the quenching responses to metalloproteins (Figure S13c,d in the Supporting Information), the ensembles based on bispyrene containing hydrophilic spacers usually exhibit larger extent responses than those containing hydrophobic spacers. Such results further prove that the spacer polarity of bispyrene probes plays a critical role in the high sensitivity and multiple responses to proteins.

Time-Resolved Emission Spectroscopy (TRES) of Bispyrene/DTAB Assemblies. The difference in sensing

DOI: 10.1021/acsami.5b06604
ACS Appl. Mater. Interfaces 2015, 7, 22487−22496

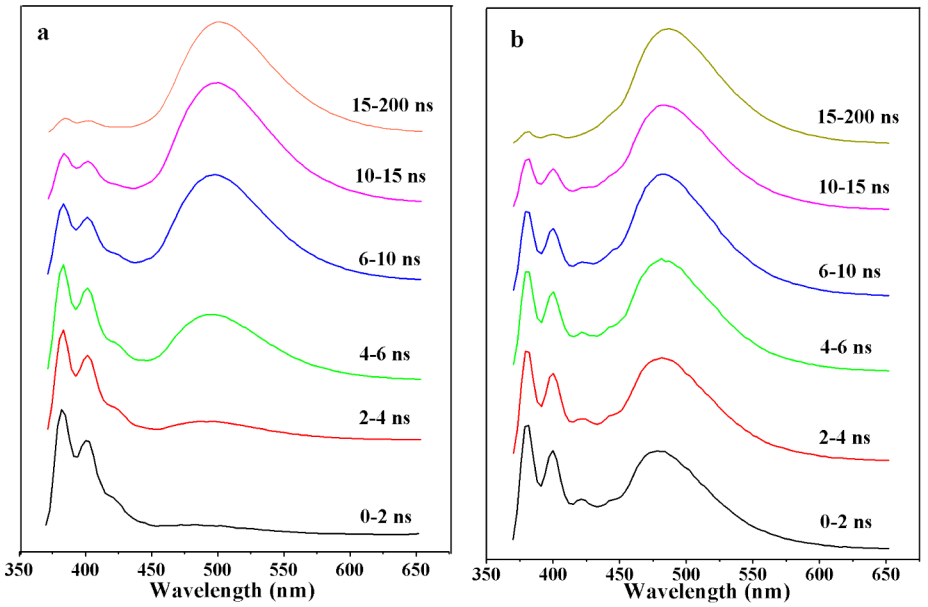

Figure 8. Time-resolved emission spectra of (a) **1**/DTAB (1.0 μM/6 mM) and (b) **2**/DTAB (1.0 μM/7 mM) in HEPES buffer solution (10 mM, pH 7.4).

behaviors of the measured fluorescent ensembles may be due to the different locations of bispyrene fluorophores in DTAB assemblies, which could be determined by their spacer polarity. Generally, pyrene molecules were found to be localized in the so-called palisade layer of the micelle, which is described as the region between the micelle surface and the micelle core.[43,44] As to the spacers of the bispyrene fluorophore, the hydrophilic one is more likely located outside the palisade layer, whereas the hydrophobic one is more possible in the hydrocarbon core of the DTAB assemblies. This assumption is verified by the TRES measurements. As shown in Figures 8 and S14 in the Supporting Information, these bispyrene/DTAB ensembles exhibit quite different excimer formation mechanisms. Excimer formation for bispyrene fluorophores with hydrophilic spacers, such as **1**, **1A**, and **1B**, is apparently time-dependent (Figures 8a and S14a,b in the Supporting Information). The absence of excimer in the early time gate (e.g., 0−4 ns) and gradual increasing of the excimer contribution in the late time gate strongly suggest that the excimer of **1**, **1A**, and **1B** is formed via Birks' scheme, where an excited monomer diffusively encounters a ground-state monomer and forms an excimer before emission.[45] Differently, the spectrum profiles of **2** and **2A** are characterized by pyrene excimer over the whole time gate (Figures 8b and S14c in the Supporting Information), indicating that the excimer of bispyrene with hydrophobic spacers forms via a preformed scheme, where the ground-state pyrene dimers are excited and decayed together.[46] Moreover, we found that the excimer formation of **1** also follows Birks' scheme in the good solvent (acetonitrile) and obeys the preformed scheme in the poor solvent (water; Figure S15 in the Supporting Information). The similarity in the excimer formation mechanism of **1**, **1A**, and **1B** in DTAB and that of **1** in the good solvent suggests that the two pyrene moieties of fluorophores with hydrophilic spacers are mobile and can move freely to form a dynamic excimer in DTAB assemblies. On the contrary, the similarity in the excimer formation of **2** and **2A** in DTAB and that of **1** in the poor solvent indicates that the two pyrene moieties locate in a restricted microenvironment and cannot move freely. Therefore, the simple difference in the polarity of the spacer connecting two pyrene moieties leads to different locations of the bispyrene fluorophore in surfactant assemblies, which further influences the sensing behaviors of the resulting fluorescent ensembles.

According to the above results and discussion, a schematic cartoon describing the protein sensing process of the present ensemble sensor and that of the control ensemble is illustrated in Scheme 2. Prior to protein addition, the bispyrene probe **1** is

Scheme 2. Cartoon Representation of the Protein Sensing Process by (a) 1/DTAB and (b) 2/DTAB Assemblies

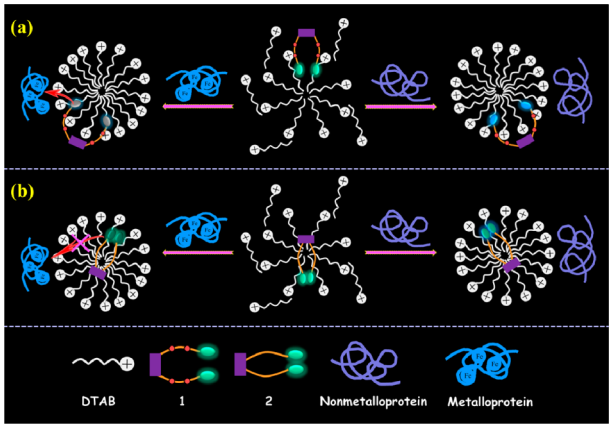

located at the palisade layer of the loosely packed DTAB assemblies, with the spacer moving flexibly (Scheme 2a). The aqueous surroundings facilitate the two pyrene moieties to form a dynamic excimer. Upon the addition of proteins, on the one hand, the added negatively charged nonmetalloproteins lead to the formation of micelle-like aggregates, and as a result, the polar spacer was stretched along the palisade layer with the two pyrene moieties separately located inside the inner layer, giving rise to monomer emission; on the other hand, the added metalloproteins induced significant fluorescence quenching because of electron/energy transfer from the assembly surface-located bispyrene probe to metal-containing cofactors.

DOI: 10.1021/acsami.5b06604
ACS Appl. Mater. Interfaces 2015, 7, 22487−22496

The quenching effect surpasses the possible ratiometric variation induced by assemble conformation changes. Differently, the control bispyrene **2**, located in the confined hydrophobic core of DTAB assemblies with preformed excimer, is less sensitive to the variation induced by the added proteins (Scheme 2b).

4. CONCLUSIONS

In summary, a fluorescent ensemble based on bispyrene **1**/DTAB assemblies could provide multiple responses to the tested proteins: ratiometric responses to nonmetalloproteins and turn-off responses to metalloproteins. The former is attributed to the electrostatic interactions between DTAB surfactants and proteins that induce different extents of aggregation variation of surfactant assemblies, which was verified by DLS and Tyndall effect measurements. The effective quenching responses to metalloproteins are ascribed to energy/electron transfer between metalloproteins and the probe. The studies with control ensembles reveal that the polarity of the spacer connecting two pyrene moieties plays an important role in locating the bispyrene fluorophores in the surfactant assemblies, which further influences the sensing process of the resulting ensemble. The present work provides a simple way of discriminating metallo- and nonmetalloproteins by providing different response modes and sheds light on the molecular design of fluorescent probes for constructing fluorescent sensing ensembles.

■ ASSOCIATED CONTENT

Supporting Information

The Supporting Information is available free of charge on the ACS Publications website at DOI: 10.1021/acsami.5b06604.

Synthesis of control compound **2**, molecular structures of control compounds, concentration effect of **1** in neat solvents, fluorescence stabilities of **1** and **1**/DTAB in HEPES buffer, fluorescence responses of control bispyrene compounds/DTAB to proteins and that of **1**/DTAB to metal ions, time-resolved fluorescence decays of **1**/DTAB to metalloproteins, DTAB concentration effect on the fluorescence emission of control compounds, time-resolved fluorescence spectra of control compounds in a DTAB solution and that of **1** in acetonitrile and water (PDF)

■ AUTHOR INFORMATION

Corresponding Author

*E-mail: dinglp33@snnu.edu.cn. Tel: 86-29-8153-0789.

Notes

The authors declare no competing financial interest.

■ ACKNOWLEDGMENTS

The authors acknowledge financial support from National Natural Science Foundation of China (21173142 and 21573140), Ministry of Education of China (NCET-12-0895), the Program of Introducing Talents of Discipline to Universities (B14041), and the Fundamental Research Funds for the Central Universities (GK201301006).

■ REFERENCES

(1) Yan, X.; Zhu, P.; Li, J. Self-Assembly and Application of Diphenylalanine-Based Nanostructures. *Chem. Soc. Rev.* **2010**, *39*, 1877−1890.

(2) Verma, G.; Hassan, P. Self Assembled Materials: Design Strategies and Drug Delivery Perspectives. *Phys. Chem. Chem. Phys.* **2013**, *15*, 17016−17028.

(3) Hu, R.; Feng, J.; Hu, D.; Wang, S.; Li, S.; Li, Y.; Yang, G. A Rapid Aqueous Fluoride Ion Sensor with Dual Output Modes. *Angew. Chem., Int. Ed.* **2010**, *49*, 4915−4918.

(4) Kumari, N.; Jha, S.; Bhattacharya, S. An Efficient Probe for Rapid Detection of Cyanide in Water at Parts per Billion Levels and Naked-Eye Detection of Endogenous Cyanide. *Chem. - Asian J.* **2014**, *9*, 830−837.

(5) Geng, J.; Goh, C. C.; Tomczak, N.; Liu, J.; Liu, R.; Ma, L.; Ng, L. G.; Gurzadyan, G. G.; Liu, B. Micelle/Silica Co-Protected Conjugated Polymer Nanoparticles for Two-Photon Excited Brain Vascular Imaging. *Chem. Mater.* **2014**, *26*, 1874−1880.

(6) Dhar, S.; Rana, D. K.; Bhattacharya, S. C. Influence of Nanoscopic Micellar Confinements on Spectroscopic Probing and Rotational Dynamics of an Antioxidative Naphthalimide Derivative. *Colloids Surf., A* **2012**, *402*, 117−126.

(7) Wang, J.; Qian, X.; Qian, J.; Xu, Y. Micelle-Induced Versatile Performance of Amphiphilic Intramolecular Charge-Transfer Fluorescent Molecular Sensors. *Chem. - Eur. J.* **2007**, *13*, 7543−7552.

(8) Xu, Y.; Li, B.; Xiao, L.; Li, W.; Zhang, C.; Sun, S.; Pang, Y. The Sphere-to-Rod Transition of Squaraine-Embedded Micelles: A Self-Assembly Platform Displays a Distinct Response to Cysteine and Homocysteine. *Chem. Commun.* **2013**, *49*, 7732−7734.

(9) Singh, Y.; Gulyani, A.; Bhattacharya, S. A New Ratiometric Fluorescence Probe as Strong Sensor of Surface Charge of Lipid Vesicles and Micelles. *FEBS Lett.* **2003**, *541*, 132−136.

(10) Rusu, A. D.; et al. Fluorescent Polymeric Aggregates for Selective Response to Sarin Surrogates. *Chem. Commun.* **2014**, *50*, 9965−9968.

(11) Mallick, A.; Mandal, M. C.; Haldar, B.; Chakrabarty, A.; Das, P.; Chattopadhyay, N. Surfactant-Induced Modulation of Fluorosensor Activity: A Simple Way to Maximize the Sensor Efficiency. *J. Am. Chem. Soc.* **2006**, *128*, 3126−3127.

(12) Ding, L.; Wang, S.; Liu, Y.; Cao, J.; Fang, Y. Bispyrene/Surfactant Assemblies as Fluorescent Sensor Platform: Detection and Identification of Cu^{2+} and Co^{2+} in Aqueous Solution. *J. Mater. Chem. A* **2013**, *1*, 8866−8875.

(13) Kumari, N.; Jha, S.; Misra, S. K.; Bhattacharya, S. A Probe for the Selective and Parts-per-Billion-Level Detection of Copper (II) and Mercury (II) Using a Micellar Medium and Its Utility in Cell Imaging. *ChemPlusChem* **2014**, *79*, 1059−1064.

(14) Bhattacharya, S.; Gulyani, A. First Report of Zn^{2+} Sensing Exclusively at Mesoscopic Interfaces. *Chem. Commun.* **2003**, 1158−1159.

(15) Kumari, N.; Dey, N.; Jha, S.; Bhattacharya, S. Ratiometric, Reversible, and Parts per Billion Level Detection of Multiple Toxic Transition Metal Ions Using a Single Probe in Micellar Media. *ACS Appl. Mater. Interfaces* **2013**, *5*, 2438−2445.

(16) Tian, H.; Qian, J.; Bai, H.; Sun, Q.; Zhang, L.; Zhang, W. Micelle-Induced Multiple Performance Improvement of Fluorescent Probes for H_2S Detection. *Anal. Chim. Acta* **2013**, *768*, 136−142.

(17) Xu, Y.; Malkovskiy, A.; Wang, Q.; Pang, Y. Molecular Assembly of a Squaraine Dye with Cationic Surfactant and Nucleotides: Its Impact on Aggregation and Fluorescence Response. *Org. Biomol. Chem.* **2011**, *9*, 2878−2884.

(18) Wang, L.; Chen, H.; Wang, H.; Wang, F.; Kambam, S.; Wang, Y.; Zhao, W.; Chen, X. A Fluorescent Probe with High Selectivity to Glutathione over Cysteine and Homocysteine Based on Positive Effect of Carboxyl on Nucleophilic Substitution in CTAB. *Sens. Actuators, B* **2014**, *192*, 708−713.

(19) Cao, J.; Ding, L.; Hu, W.; Chen, X.; Chen, X.; Fang, Y. Ternary System Based on Fluorophore−Surfactant Assemblies Cu^{2+} for Highly Sensitive and Selective Detection of Arginine in Aqueous Solution. *Langmuir* **2014**, *30*, 15364−15372.

(20) Zhang, L.; Zhao, C.; Zhou, J.; Kondo, T. Fluorescent Micelles Based on Hydrophobically Modified Cationic Cellulose for Sensing

DOI: 10.1021/acsami.5b06604
ACS Appl. Mater. Interfaces 2015, 7, 22487−22496

Trace Explosives in Aqueous Solutions. *J. Mater. Chem. C* **2013**, *1*, 5756−5764.
(21) Ding, L.; Bai, Y.; Cao, Y.; Ren, G.; Blanchard, G. J.; Fang, Y. Micelle-Induced Versatile Sensing Behavior of Bispyrene-Based Fluorescent Molecular Sensor for Picric Acid and PYX Explosives. *Langmuir* **2014**, *30*, 7645−7653.
(22) Dey, N.; Samanta, S. K.; Bhattacharya, S. Selective and Efficient Detection of Nitro-Aromatic Explosives in Multiple Media including Water, Micelles, Organogel, and Solid Support. *ACS Appl. Mater. Interfaces* **2013**, *5*, 8394−8400.
(23) Xu, Q.; Wu, C.; Zhu, C.; Duan, X.; Liu, L.; Han, Y.; Wang, Y.; Wang, S. A Water-Soluble Conjugated Polymer for Protein Identification and Denaturation Detection. *Chem. - Asian J.* **2010**, *5*, 2524−2529.
(24) Miranda, O. R.; You, C.-C.; Phillips, R.; Kim, I.-B.; Ghosh, P. S.; Bunz, U. H.; Rotello, V. M. Array-Based Sensing of Proteins Using Conjugated Polymers. *J. Am. Chem. Soc.* **2007**, *129*, 9856−9857.
(25) Muthuraj, B.; Hussain, S.; Iyer, P. K. A Rapid and Sensitive Detection of Ferritin at a Nanomolar Level and Disruption of Amyloid β Fibrils Using Fluorescent Conjugated Polymer. *Polym. Chem.* **2013**, *4*, 5096−5107.
(26) Sandanaraj, B. S.; Demont, R.; Thayumanavan, S. Generating Patterns for Sensing Using a Single Receptor Scaffold. *J. Am. Chem. Soc.* **2007**, *129*, 3506−3507.
(27) Savariar, E. N.; Ghosh, S.; Thayumanavan, S. Disassembly of Noncovalent Amphiphilic Polymers with Proteins and Utility in Pattern Sensing. *J. Am. Chem. Soc.* **2008**, *130*, 5416−5417.
(28) González, D. C.; Savariar, E. N.; Thayumanavan, S. Fluorescence Patterns from Supramolecular Polymer Assembly and Disassembly for Sensing Metallo- and Nonmetalloproteins. *J. Am. Chem. Soc.* **2009**, *131*, 7708−7716.
(29) Azagarsamy, M. A.; Yesilyurt, V.; Thayumanavan, S. Disassembly of Dendritic Micellar Containers Due to Protein Binding. *J. Am. Chem. Soc.* **2010**, *132*, 4550−4551.
(30) Jia, L.; Xu, L.; Wang, Z.; Xu, J.; Ji, J. Label-Free Fluorescent Sensor for Probing Heparin-Protein Interaction Based on Supramolecular Assemblies. *Chin. J. Chem.* **2014**, *32*, 85−90.
(31) Hu, W.; Ding, L.; Cao, J.; Liu, L.; Wei, Y.; Fang, Y. Protein Binding-Induced Surfactant Aggregation Variation: A New Strategy of Developing Fluorescent Aqueous Sensor for Proteins. *ACS Appl. Mater. Interfaces* **2015**, *7*, 4728−4736.
(32) Ezzell, S. A.; McCormick, C. L. Synthesis and Solution Characterization of Pyrene-Labeled Polyacrylamides. In *Water-Soluble Polymers: Synthesis, Solution Properties, and Applications*; Shalaby, S. W., McCormick, C. L., Butler, G. B., Eds.; American Chemical Society: Washington, DC, 1991.
(33) Ding, L.; Liu, Y.; Cao, Y.; Wang, L.; Xin, Y.; Fang, Y. A Single Fluorescent Self-Assembled Monolayer Film Sensor with Discriminatory Power. *J. Mater. Chem.* **2012**, *22*, 11574−11582.
(34) Ni, X.-L.; Wang, S.; Zeng, X.; Tao, Z.; Yamato, T. Pyrene-Linked Triazole-Modified Homooxacalix[3]arene: A Unique C_3 Symmetry Ratiometric Fluorescent Chemosensor for Pb^{2+}. *Org. Lett.* **2011**, *13*, 552−555.
(35) Sanghamitra, N. J.; Ueno, T. Expanding Coordination Chemistry from Protein to Protein Assembly. *Chem. Commun.* **2013**, *49*, 4114−4126.
(36) Cao, Y.; Ding, L.; Hu, W.; Peng, J.; Fang, Y. A Surfactant-Modulated Fluorescent Sensor with Pattern Recognition Capability: Sensing and Discriminating Multiple Heavy Metal Ions in Aqueous Solution. *J. Mater. Chem. A* **2014**, *2*, 18488−18496.
(37) Sandanaraj, B. S.; Demont, R.; Aathimanikandan, S. V.; Savariar, E. N.; Thayumanavan, S. Selective Sensing of Metalloproteins from Nonselective Binding Using a Fluorogenic Amphiphilic Polymer. *J. Am. Chem. Soc.* **2006**, *128*, 10686−10687.
(38) Kim, I.-B.; Dunkhorst, A.; Bunz, U. H. Nonspecific Interactions of a Carboxylate-Substituted PPE with Proteins. A Cautionary Tale for Biosensor Applications. *Langmuir* **2005**, *21*, 7985−7989.
(39) Davis, B. W.; Niamnont, N.; Hare, C. D.; Sukwattanasinitt, M.; Cheng, Q. Nanofibers Doped with Dendritic Fluorophores for Protein Detection. *ACS Appl. Mater. Interfaces* **2010**, *2*, 1798−1803.
(40) Yuan, Z.; Du, Y.; Tseng, Y.-T.; Peng, M.; Cai, N.; He, Y.; Chang, H.-T.; Yeung, E. S. Fluorescent Gold Nanodots Based Sensor Array for Proteins Discrimination. *Anal. Chem.* **2015**, *87*, 4253−4259.
(41) Lakowicz, J. R. *Principles of Fluorescence Spectroscopy*, 2nd ed.; Springer: New York, 2006.
(42) Pu, K.-Y.; Liu, B. Fluorescence Turn-on Responses of Anionic and Cationic Conjugated Polymers toward Proteins: Effect of Electrostatic and Hydrophobic Interactions. *J. Phys. Chem. B* **2010**, *114*, 3077−3084.
(43) Cuomo, F.; Palazzo, G.; Ceglie, A.; Lopez, F. Quenching Efficiency of Pyrene Fluorescence by Nucleotide Monophosphates in Cationic Micelles. *J. Photochem. Photobiol., A* **2009**, *202*, 21−27.
(44) Yan, H.; Cui, P.; Liu, C.-B.; Yuan, S.-L. Molecular Dynamics Simulation of Pyrene Solubilized in a Sodium Dodecyl Sulfate Micelle. *Langmuir* **2012**, *28*, 4931−4938.
(45) Chen, S.; Duhamel, J.; Winnik, M. A. Probing End-to-End Cyclization beyond Willemski and Fixman. *J. Phys. Chem. B* **2011**, *115*, 3289−3302.
(46) Murata, K.; Aoki, M.; Suzuki, T.; Harada, T.; Kawabata, H.; Komori, T.; Ohseto, F.; Ueda, K.; Shinkai, S. Thermal and Light Control of the Sol-Gel Phase Transition in Cholesterol-Based Organic Gels. Novel Helical Aggregation Modes as Detected by Circular Dichroism and Electron Microscopic Observation. *J. Am. Chem. Soc.* **1994**, *116*, 6664−6676.

DOI: 10.1021/acsami.5b06604
ACS Appl. Mater. Interfaces 2015, 7, 22487−22496